Journal of Organometallic Chemistry, 361 (1989) 109–116
Elsevier Sequoia S.A., Lausanne – Printed in The Netherlands

Synthesis and some reactions of $Fe(CO)_2(dppe)(SR)_2$ and $Fe_3(CO)_6(SAr)_6$ complexes. The crystal structure of *cis,cis,cis*-$Fe(CO)_2(dppe)(SPh)_2$

János Takács, László Markó *,

Research Group for Petrochemistry of the Hungarian Academy of Sciences, H-8200 Veszprém (Hungary)

and László Párkányi

Central Research Institute of Chemistry of the Hungarian Academy of Sciences, H-1525-Budapest, P.O. Box 17 (Hungary)

(Received March 28th, 1988)

Abstract

The complexes $Fe(CO)_2(dppe)(SR)_2$ (dppe = $Ph_2PCH_2CH_2PPh_2$; R = s-Bu, Ph, p-C_6H_4Me, p-C_6H_4OMe, p-$C_6H_4NHC(O)Me$) have been synthesized from Fe^{2+} salts by treatment with CO in the presence of dppe and RS^- and the crystal structure of the $Fe(CO)(dppe)(SPh)_2$ derivative has been determined. The ligands occupy *cis,cis,cis* positions and there are two enantiomeric molecules in the asymmetric unit (space group $P\bar{1}$) of the crystal. The $Fe(CO)_2(dppe)(SR)_2$ complexes form 1/2 adducts with $HgCl_2$. In the absence of dppe, methanol solutions of Fe^{2+} and ArS^- (1/2; Ar = Ph, p-C_6H_4Me, p-C_6H_4OMe) take up CO to give the trinuclear thiolato complexes $Fe_3(CO)_6(SAr)_6$.

Introduction

There has been increasing interest in the study of absorption of small molecules such as O_2, N_2, CO, and C_2H_4, by transition metal complexes in recent years [1–5]. In continuation of our studies of the reactions of sulfur-containing iron compounds with CO under mild conditions [6], we have synthesized $Fe(CO)_2(dppe)(SR)_2$ (dppe = $Ph_2PCH_2CH_2PPh_2$) and $Fe_3(CO)_6(SAr)_6$ complexes from iron(II) salts by uptake of CO in the presence of RS^-, studied some of their reactions, and determined the crystal structure of the *cis,cis,cis*-$Fe(CO)_2(dppe)(SPh)_2$ derivative (**1**).

Results

The complex $Fe(CO)_2(dppe)(SPh)_2$ (**1**) was first prepared by Haines et al. in 1972 [7] by the route shown in eq. 1.

$$Fe_2(CO)_6(SPh)_2 + 2.5\ dppe \xrightarrow[\text{xylene}]{\text{reflux}} Fe(CO)_2(dppe)(SPh)_2 \quad (1)$$

However, up to now no one has determined its crystal structure, or synthesized other thiolato derivatives. On the basis of its IR spectrum Haines proposed a structure in which two CO groups occupy *cis* positions of the octahedra, but the positions of the thiolato ligands (*cis* or *trans*) remained unknown and the possibility of obtaining optical isomers has not been examined. To prepare $Fe(CO)_2(dppe)$-$(SPh)_2$ complexes we employed treatment of iron(II) salts with CO under appropriate conditions (eq. 2).

$$Fe^{2+} + dppe + 2RS^- \xrightarrow[\text{MeOH, 25°C}]{\text{1 bar CO}} Fe(CO)_2(dppe)(SR)_2 \quad (2)$$

Carbon monoxide uptake was fast and stoichiometric. Complex **1** and the new R = s-Bu, p-C_6H_4Me, p-C_6H_4OMe, p-$C_6H_4NHC(O)Me$ derivatives showed IR spectra in the $\nu(CO)$ region which could be assigned to a single *cis*-CO isomer, and the compounds were easily isolated. In the case of less bulky thiols, such as EtSH and n-BuSH, the carbonyl bands in the IR spectra of the resulting solutions indicated that they contained a mixture of compounds, and the desired complexes could not be obtained in pure crystalline form. In the case of t-BuSH no CO absorption took place, probably for steric reasons. The IR data for the $Fe(CO)_2(dppe)(SR)_2$ complexes are shown in Table 1.

The reactions of $Fe(CO)_2(dppe)I_2$ with RS^- anions also gave the $Fe(CO)_2(dppe)$-$(SR)_2$ complexes, but this method was less convenient and yielded isomerically less pure products, probably because of the facile shift in the isomer equilibrium of the starting $Fe(CO)_2(dppe)I_2$ in solution [8]. It should be mentioned that the $Fe(CO)_2(dppe)(SPh)_2$ isomer prepared by Haines and that we obtained gave identical IR spectra.

It is of interest that the MeOH solution of Fe^{2+}/RS^- (1/2) (R = alkyl and aryl) absorbed CO even in the abscene of dppe, and initially gave unidentified iron carbonyls (IR evidence) that we have not yet isolated in crystalline form. In the case of aryl thiolates, when the MeOH solutions of these species were kept under CO for 2–3 days dark green precipitates were formed and were characterized by IR spectroscopy and elemental analysis as $Fe_3(CO)_6(SAr)_6$ (Ar = Ph, p-C_6H_4Me, p-C_6H_4OMe). The phenyl derivative has been prepared previously from $Fe(CO)_5$ and PhSSPh [9], and its structure is known [10]; the three iron atoms are connected by bridging thiolato groups and the central iron atom does not bear a CO ligand: i.e. it is $(OC)_3Fe(\mu\text{-SPh})_3Fe(\mu\text{-SPh})_3Fe(CO)_3$. Table 1 lists the IR data for these trinuclear complexes, and eq. 3 shows the overall reaction leading to the formation of $Fe_3(CO)_6(SAr)_6$ compounds under the conditions we used:

$$3Fe^{2+} + 6ArS^- + 6CO \xrightarrow[\text{3 days, MeOH}]{\text{20°C}} Fe_3(CO)_6(SAr)_6 \quad (3)$$

Attempts to isolate the corresponding alkyl derivatives $Fe_3(CO)_6(SR)_6$ were unsuccessful.

Table 1

IR data

R or Ar	ν(CO) cm^{-1} (in CH_2Cl_2)		
$Fe(CO)_2(dppe)(SR)_2$ complexes			
Et	2019 m,sh	2007.5 s	1955 s
	1944 s	1939 m,sh	
n-Bu	2019 m,sh	2005.5 s	1968 s,sh
	1954.5 s	1947 s,sh	
s-Bu	2005 s	1954.5 s	
Ph	2017 s	1970 s	
p-C_6H_4Me	2016.5 s	1968 s	
p-C_6H_4OMe	2015 s	1966.5 s	
p-$C_6H_4NHC(O)Me$	2017 s	1969 s	
$Fe_3(CO)_6(SAr)_6$ complexes			
Ph	2082 s	2032.5 m,br	
p-C_6H_4Me	2080 s	2029 m,br	
p-C_6H_4OMe	2077.5 s	2027 m,br	
$Fe(CO)_2(dppe)(SR)_2 \cdot 2HgCl_2$ adducts			
s-Bu	2056 s	1996 s	
Ph	2062 s	2008 s	
p-C_6H_4Me	2055 s	2002.5 s	
p-C_6H_4OMe	2062.5 s	2008 s	
p-$C_6H_4NHC(O)Me$	2053 s	1996 s	

The crystal structure of cis,cis,cis-$Fe(CO)_2(dppe)(SPh)_2$ (1)

The asymmetric unit contains two molecules (**A** and **B**) which constitute two enantiomeric forms of the chiral $FeA_2B_2C_2$ octahedron. Molecule **A** of the asym-

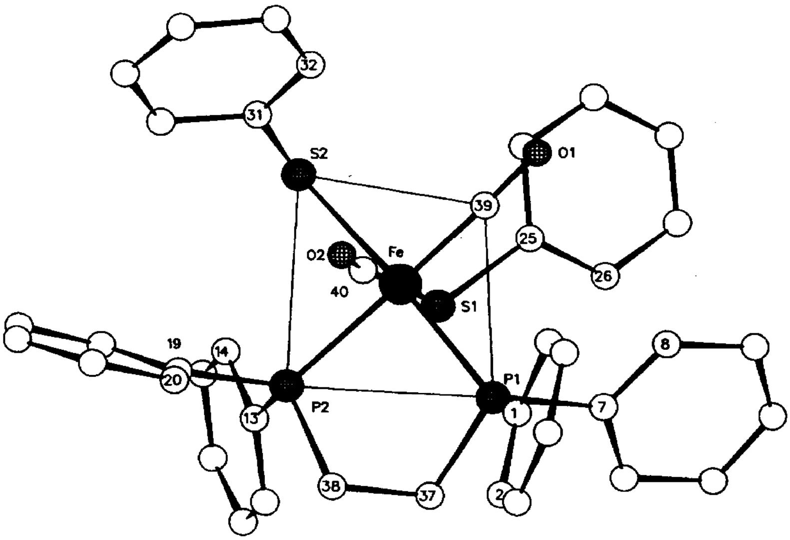

Fig. 1. The molecular diagram of molecule A of the asymmetric unit of 1, with the numbering of atoms. Numbers are for carbon atoms unless indicated otherwise. Only the bridgehead carbon atom and one connecting carbon atom are labeled for the phenyl rings. The thin lines connect ligands in the equatorial plane of the iron atom.

metric unit is depicted in Fig. 1; the two CO, SPh and PPh_2 ligands occupy *cis*-positions. Bond distances and angles (Table 2) are normal, and the limited accuracy of the data precludes further discussion.

Reactions of $Fe(CO)_2(dppe)(SR)_2$ with $HgCl_2$

The complexes $Fe(CO)_2(dppe)(SR)_2$ (R = s-Bu, Ph, p-C_6H_4Me, p-C_6H_4OMe, p-$C_6H_4NHC(O)Me$) react with $HgCl_2$ in solution to yield yellow microcrystalline solids, which are unstable at room temperature. Their elemental analysis indicates that they contain two molecules of $HgCl_2$ to one of $Fe(CO)_2(dppe)(SR)_2$, but they decompose rapidly at 25 °C to give non-carbonyl compounds that were not further studied.

The ν(CO) absorption bands in the IR spectra of $Fe(CO)_2(dppe)(SR)_2 \cdot 2HgCl_2$ adducts are at ca. 30–50 cm^{-1} higher wavenumbers than those for the parent $Fe(CO)_2(dppe)(SR)_2$ complexes (Table 1). These IR characteristics make it unlikely that a direct Fe–Hg bond is present, since in that case one would expect a larger $\Delta\nu$(CO) shift toward higher wavenumbers (70–120 cm^{-1}) [11,12]. A seven-coordinate Fe atom is also not very probable. The shift of the ν(CO) band is, however, larger than the shift observed upon formation of $L_2(CO)_2FeX_2 \cdot HgCl_2$ adducts ($\Delta\nu$(CO) ~ 20 cm^{-1} [12]), in which the mercury atom bridges the halogens of $L_2(CO)_2FeX_2$. We thus prefer a structure in which the electron deficient Hg atoms are bonded to the "mercurophilic" sulfur atom:

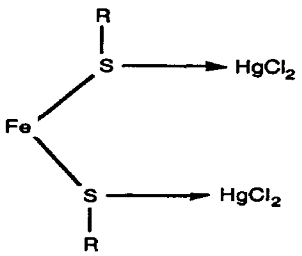

Adducts of $Fe(CO)_2(dppe)(SR)_2$ complexes with other Hg halides and Lewis acids [e.g. $(THF)Cr(CO)_5$, $(THF)W(CO)_5$] were detected by IR spectroscopy, but owing to their low stabilities, they could not be isolated in crystalline form.

Experimental

All preparations were carried out under pure CO or Ar. Elemental analysis of the new compounds gave satisfactory results, except for the unstable $Fe(CO)_2(dppe)$-$(SR)_2 \cdot 2HgCl_2$ adducts.

$Fe(CO)_2(dppe)(SR)_2$. To a mixture of 278 mg (1.0 mmol) $FeSO_4 \cdot 7H_2O$ and 398 mg (1.0 mmol) dppe in 20 ml MeOH, a MeOH solution (10 ml) of 2.0 mmol RSH and 108 mg (2.0 mmol) NaOMe was added dropwise with stirring under CO. The phosphine gradually dissolved, and the solution became red as the two equivalents of CO were absorbed. In the case of R = s-Bu, Ph, p-C_6H_4Me, p-C_6H_4OMe the product separated, together with Na_2SO_4, as a red powder. After 5 h of stirring the MeOH was pumped off and the residue extracted with CH_2Cl_2 (2 × 15 ml). The combined CH_2Cl_2 extracts were filtered to remove Na_2SO_4, then concentrated in

Table 2

Relevant bond distances (Å) and angles (deg.) with their esd's for 1. The first line of data in each case refers to molecule A, and the second to molecule B

Bond distances					
Fe–P(1)	2.232(4)	Fe–P(2)	2.294(5)	Fe–S(1)	2.339(5)
	2.249(4)		2.281(4)		2.350(4)
Fe–S(2)	2.343(4)	Fe–C(39)	1.736(15)	Fe–C(40)	1.769(15)
	2.346(5)		1.756(16)		1.782(13)
P(1)–C(1)	1.818(14)	P(1)–C(7)	1.793(14)	P(1)–C(37)	1.834(15)
	1.780(14)		1.818(14)		1.798(15)
P(2)–C(13)	1.818(15)	P(2)–C(19)	1.810(13)	P(2)–C(38)	1.812(13)
	1.803(15)		1.816(14)		1.862(12)
S(1)–C(25)	1.780(14)	S(2)–C(31)	1.769(14)	O(1)–C(39)	1.127(17)
	1.750(15)		1.791(15)		1.149(20)
O(2)–C(40)	1.102(18)	C(37)–C(38)	1.499(21)		
	1.096(16)		1.505(20)		

Bond angles			
P(1)–Fe–P(2)	86.2(1)	P(1)–Fe–S(1)	86.7(2)
	86.7(1)		86.6(2)
P(1)–Fe–S(2)	172.7(2)	P(1)–Fe–C(39)	94.8(5)
	173.3(2)		96.9(4)
P(1)–Fe–C(40)	94.9(4)	P(2)–Fe–S(1)	86.9(2)
	93.8(4)		86.3(2)
P(2)–Fe–S(2)	89.4(2)	P(2)–Fe–C(3)	179.0(5)
	90.0(2)		176.0(4)
P(2)–Fe–C(40)	89.1(5)	S(1)–Fe–S(2)	87.2(2)
	90.9(5)		87.4(2)
S(1)–Fe–C(39)	93.5(5)	S(1)–Fe–C(40)	175.5(6)
	92.1(5)		177.2(5)
S(20–Fe–C(39)	98.7(5)	S(2)–Fe–C(40)	90.9(4)
	86.3(4)		92.1(4)
C(39)–Fe–C(40)	90.6(7)	Fe–P(1)–C(1)	114.4(5)
	90.6(7)		120.2(4)
Fe–P(1)–C(7)	120.5(4)	Fe–P(1)–C(37)	106.1(4)
	114.2(4)		104.9(4)
C(1)–P(1)–C(7)	104.3(7)	C(1)–P(1)–C(37)	105.2(6)
	104.3(7)		107.3(6)
C(7)–P(1)–C(37)	105.2(6)	Fe–P(2)–C(13)	119.5(4)
	105.0(6)		119.7(5)
Fe–P(2)–C(19)	118.8(5)	Fe–P(2)–C(38)	105.0(5)
	117.4(5)		105.3(5)
C(13)–P(2)–C(19)	105.1(6)	C(13)–P(2)–C(38)	103.2(6)
	103.6(7)		104.8(6)
C(19)–P(2)–C(38)	102.9(6)	Fe–S(1)–C(25)	112.4(5)
	104.4(6)		114.9(5)
Fe–S(2)–C(31)	109.5(5)	P(1)–C(37)–C(38)	108.0(9)
	107.7(5)		110.4(9)
P(2)–C(38)–C(37)	107.4(8)	Fe–C(39)–O(1)	175.9(12)
	104.8(8)		174.9(12)
Fe–C(40)–O(2)	174.5(12)		
	178.2(13)		

vacuo. Addition of hexane and cooling to $-18°C$ yielded the product as a red microcrystalline solid. Larger crystals were obtained from CH_2Cl_2/hexane by the slow diffusion method.

Yields: R = s-Bu 392 mg (57%), Ph 444 mg (61%), p-C_6H_4Me 498 mg (66%), p-C_6H_4OMe 520 mg (66%), p-$C_6H_4NHC(O)Me$ 560 mg (67%).

$Fe(CO)_2(dppe)(SR)_2 \cdot 2HgCl_2$. Saturated THF solutions of $Fe(CO)_2(dppe)(SR)_2$ and a large excess of $HgCl_2$ were mixed under CO. The mixture immediately became yellow, and a yellow microcrystalline precipitate formed rapidly. This was filtered off, washed with a small amount of THF, and dried in vacuo for a short time.

$Fe(CO)_2(dppe)(S\text{-}Bu^s)_2 \cdot 2HgCl_2$. Found: C, 36.2; H, 3.68; Cl, 11.38. $C_{36}H_{42}FeHg_2Cl_4O_2P_2S_2$, (Mw 1231.6) calc.: C, 35.10; H, 3.43; Cl, 11.51%.

$Fe(CO)_2(dppe)(SPh)_2 \cdot 2HgCl_2$. Found: C, 38.3; H, 2.82; Cl, 8.63. $C_{40}H_{34}FeHg_2Cl_4O_2P_2S_2$ (Mw 1271.7) calc.: C, 37.77; H, 2.69; Cl, 10.85%.

$Fe(CO)_2(dppe)(SC_6H_4OMe)_2 \cdot 2HgCl_2$. Found: C, 40.2; H, 3.3; Cl, 9.02. $C_{42}H_{38}FeHg_2Cl_4O_4P_2S_2$ (Mw 1331.6) calc.: C, 37.88; H, 2.88; Cl, 10.64%.

$Fe_3(CO)_6(SAr)_6$. ArSH (Ar = Ph, p-C_6H_4Me, p-C_6H_4OMe) (8.0 mmol) and 8.0 mmol (432 mg) NaOMe were dissolved in 30 ml MeOH saturated with CO. This solution was added with stirring under CO to a MeOH solution (30 ml) of 4.0 mmol (1112 mg) $FeSO_4 \cdot 7H_2O$ in a 200 ml Schlenk tube. As the stirring of the dark green

Table 3

Crystal data, data collection and least-squares parameters for **1**

Empirical formula	$C_{40}H_{34}O_2S_2P_2Fe$
M (a.m.u.)	728.6
a (Å)	11.490(10)
b (Å)	16.666(8)
c (Å)	19.387(5)
α (deg.)	85.32(3)
β (deg.)	97.17(6)
γ (deg.)	105.32(8)
V (Å^3)	3549(7)
Space group	$P\bar{1}$
Z	4
$F(000)$	1512
D_c (gcm^{-3})	1.363
λ(Mo-$K\alpha$) (Å)	0.71069
μ(Mo-$K\alpha$) (cm^{-1})	6.59
2θ limits (deg.)	3–40
Scan technique	θ–2θ
No. of reflections collected	12466
No. of unique data	12334
No. of reflections used in least-squares (NO)	2419 [$I \geq 3\sigma(I)$]
No. of variables (NV)	425
Weighting scheme	$w = 4F_0^2/\sigma(F_0^2)^2$
R_0	0.056
R_w	0.052
$(\Sigma w(\lvert F_0 \rvert - \lvert F_c \rvert)^2/(NO - NV))^{1/2}$	1.993
Approx. crystal size (mm)	0.09×0.10×0.20

Table 4

Atomic coordinates and B_{eq} ($Å^2$) values [a] for the non-hydrogen atoms of **1**, with esd's

Atom	Molecule A				Molecule B			
	x/a	y/b	z/c	B_{eq}	x/a	y/b	z/c	B_{eq}
Fe	0.1123(2)	0.1147(1)	0.2755(2)	2.9(2)	0.3753(2)	0.3910(1)	0.7722(1)	2.7(2)
P(1)	0.1480(3)	0.2536(2)	0.2628(2)	2.9(4)	0.1817(4)	0.3135(2)	0.7610(2)	2.8(4)
P(2)	0.3005(3)	0.1321(2)	0.2394(2)	2.8(4)	0.4244(3)	0.2806(2)	0.7313(2)	2.6(4)
S(1)	0.0368(3)	0.1119(2)	0.1577(2)	3.6(4)	0.3407(4)	0.4350(2)	0.6549(2)	3.2(4)
S(2)	0.0807(4)	−0.0305(2)	0.2741(2)	4.5(4)	0.5768(4)	0.4706(3)	0.7698(2)	4.0(5)
O(1)	−0.1198(8)	0.0884(6)	0.3252(5)	5.7(11)	0.3319(8)	0.5377(6)	0.8253(6)	5.0(11)
O(2)	−0.2124(9)	0.1097(6)	0.4184(5)	6.5(12)	0.4234(9)	0.3331(6)	0.9142(5)	5.1(12)
C(1)	0.1899(12)	0.3070(7)	0.3440(7)	4.2(16)	0.0636(11)	0.3588(8)	0.7221(7)	2.3(14)
C(2)	0.2981(12)	0.3723(8)	0.3543(7)	5.9(16)	0.0446(14)	0.4275(9)	0.7483(8)	4.7(18)
C(3)	0.3286(13)	0.4084(9)	0.4173(8)	5.4(18)	−0.0452(14)	0.4638(9)	0.7183(9)	5.1(19)
C(4)	0.2563(13)	0.3825(8)	0.4705(8)	5.1(18)	−0.1219(14)	0.4292(10)	0.6626(9)	5.7(10)
C(5)	0.1512(13)	0.3200(9)	0.4612(8)	5.6(18)	−0.1050(13)	0.3622(9)	0.6344(8)	5.2(18)
C(6)	0.1171(12)	0.2815(8)	0.3982(7)	4.0(15)	−0.0141(13)	0.3249(9)	0.6640(8)	4.6(18)
C(7)	0.0362(11)	0.3009(8)	0.2161(7)	5.5(15)	0.1280(11)	0.2633(8)	0.8421(7)	2.8(15)
C(8)	−0.0724(13)	0.2871(9)	0.2396(7)	4.9(17)	0.0888(12)	0.1770(9)	0.8525(7)	3.8(16)
C(9)	−0.1660(14)	0.3214(10)	0.2037(8)	6.5(20)	0.0522(13)	0.1416(9)	0.9164(8)	4.4(17)
C(10)	−0.1407(13)	0.3687(9)	0.1447(8)	5.6(18)	0.0576(13)	0.1903(10)	0.9705(8)	4.6(18)
C(11)	−0.0330(13)	0.3851(9)	0.1193(8)	5.8(18)	0.0940(13)	0.2752(10)	0.9608(8)	5.0(18)
C(12)	0.0612(13)	0.3510(9)	0.1557(8)	5.2(17)	0.1268(13)	0.3117(9)	0.8963(8)	5.0(19)
C(13)	0.3126(11)	0.1128(7)	0.1499(7)	3.1(14)	0.4609(11)	0.2857(8)	0.6430(7)	2.6(15)
C(14)	0.2509(11)	0.0328(8)	0.1249(7)	3.7(15)	0.5468(12)	0.3529(8)	0.6175(7)	3.4(16)
C(15)	0.2566(13)	0.0172(8)	0.0577(7)	4.8(17)	0.5786(13)	0.3563(9)	0.5510(7)	3.8(17)
C(16)	0.3130(12)	0.0782(9)	0.0127(7)	4.6(16)	0.5233(15)	0.2936(10)	0.5085(8)	5.4(20)
C(17)	0.3694(13)	0.1562(9)	0.0350(8)	5.6(18)	0.4384(15)	0.2282(10)	0.5298(8)	5.6(20)
C(18)	0.3681(11)	0.1738(7)	0.1043(7)	3.6(15)	0.4028(13)	0.2225(9)	0.5974(8)	4.4(18)
C(19)	0.4081(11)	0.0839(7)	0.2917(7)	3.5(15)	0.5444(12)	0.2420(8)	0.7817(7)	3.6(16)
C(20)	0.4574(14)	0.1117(9)	0.3568(8)	6.0(19)	0.6549(13)	0.2542(9)	0.7564(8)	4.4(18)
C(21)	0.5341(14)	0.0716(9)	0.4002(8)	6.5(20)	0.7499(14)	0.2278(10)	0.7964(9)	5.7(19)
C(22)	0.5606(14)	0.0060(9)	0.3775(8)	6.3(20)	0.7307(13)	0.1890(9)	0.8595(8)	5.2(19)
C(23)	0.5086(14)	−0.0264(9)	0.3143(9)	6.6(21)	0.6225(14)	0.1749(10)	0.8855(8)	5.0(19)
C(24)	0.4332(13)	0.0156(9)	0.2703(8)	5.7(19)	0.5260(12)	0.2022(9)	0.8457(8)	4.2(17)
C(25)	−0.1237(12)	0.0955(8)	0.1450(7)	3.9(16)	0.2849(12)	0.5240(8)	0.6413(7)	3.2(16)
C(26)	−0.1702(12)	0.1515(8)	0.1043(7)	4.3(16)	0.3540(14)	0.6006(9)	0.6670(8)	4.6(18)
C(27)	−0.2982(13)	0.1372(9)	0.0897(8)	5.3(17)	0.3101(14)	0.6719(9)	0.6506(8)	5.5(20)
C(28)	−0.3690(12)	0.0687(9)	0.1189(8)	5.2(17)	0.2043(14)	0.6661(9)	0.6065(8)	4.8(18)
C(29)	−0.3222(12)	0.0124(8)	0.1602(8)	5.0(17)	0.1402(14)	0.5912(10)	0.5802(8)	5.4(18)
C(30)	−0.2016(12)	0.0231(8)	0.1727(7)	4.7(16)	0.1780(14)	0.5205(9)	0.5947(8)	5.0(19)
C(31)	0.1003(12)	−0.0725(8)	0.3603(7)	4.0(15)	0.6480(13)	0.4752(8)	0.8575(8)	4.1(17)
C(32)	0.0286(13)	−0.0716(9)	0.4101(8)	5.7(18)	0.7373(15)	0.4330(10)	0.8757(9)	5.9(21)
C(33)	0.0462(15)	−0.1058(10)	0.4745(9)	7.6(22)	0.7968(16)	0.4396(11)	0.9439(10)	7.5(23)
C(34)	0.1456(15)	−0.1407(9)	0.4910(9)	7.2(21)	0.7691(15)	0.4896(11)	0.9869(9)	7.1(22)
C(35)	0.2174(14)	−0.1448(10)	0.445(9)	7.2(21)	0.6832(16)	0.5323(10)	0.9701(9)	6.3(22)
C(36)	0.2001(13)	−0.1092(9)	0.3769(8)	6.0(19)	0.6198(14)	0.5252(9)	0.9033(8)	5.2(20)
C(37)	0.2817(13)	0.2893(7)	0.2148(7)	4.4(17)	0.1822(11)	0.2290(8)	0.7087(7)	3.3(15)
C(38)	0.3730(12)	0.2428(8)	0.2453(7)	4.0(16)	0.2864(12)	0.1918(8)	0.7351(7)	3.5(16)
C(39)	−0.0301(12)	0.0997(9)	0.3034(7)	4.2(14) [a]	0.3465(12)	0.4805(9)	0.8014(7)	3.5(15) [b]
C(40)	0.1790(13)	0.1142(7)	0.3628(8)	4.6(16) [a]	0.4048(13)	0.3539(8)	0.8598(7)	3.9(17) [b]

[a] B_{eq} is defined as 4/3 trace (BG), where B is the thermal motion tensor and G is the direct metric tensor. [b] Isotropic.

solution was continued all day, CO was absorbed and the colour changed to dark red. The solution was left standing overnight under CO. The same procedures were repeated next day and night. On the third day, after several hours of standing under CO the dark precipitate (containing the complex, Na_2SO_4 and decomposition products) was filtered off in vacuo. The solid was extracted several times with small amounts of CH_2Cl_2 until the filtrate was no longer green. The combined CH_2Cl_2 fractions were concentrated in vacuo. Addition of hexane and cooling to $-18\,^\circ C$ yielded dark (olive) green crystals, which were recrystallized from CH_2Cl_2/hexane. Yield: Ar = Ph 500 mg (38%); p-C_6H_4Me 214 mg (15%); p-C_6H_4OMe 452 mg (29%).

Crystal structure analysis

Details of crystal data, data collection, and least-squares parameters are given in Table 3. Because two molecules were present in the asymmetric unit, attempts were made to assign a higher space group symmetry. Cell reduction calculations failed to give a cell other than triclinic, and the space group finally was verified by least-squares refinement. Owing to the small crystal size and rather poor quality, the intensities of 4070 reflections were measured as zero or less than zero.

The structure was solved by direct methods [13], which gave the positions of both iron and all sulfur and phosphorus atoms ($R = 0.26$). Other non-hydrogen atoms were located by subsequent Fourier syntheses. The non-hydrogen atoms were refined by full-matrix anisotropic least-squares, except for the four carbonyl carbon atoms, which yielded non-positive definite thermal parameters. Isotropic temperature factors were, therefore, retained in the refinement for these atoms. Hydrogen atomic positions were placed in calculated positions and not refined. No absorption correction was applied. Atomic scattering factors were taken from ref. 14. Final atomic parameters for the non-hydrogen atoms are listed in Table 4.

References

1 H. Buttner and R.D. Feltham, Inorg. Chem., 11 (1972) 971.
2 D. Sellmann, P. Kreutzer and E. Unger, Z. Naturforsch. B, 33 (1978) 190.
3 C.A. McAuliffe, D.S. Barratt, C.G. Benson, A. Hosseini, M.G. Little and K. Minten, J. Organomet. Chem., 258 (1983) 35.
4 C.A. Koval, R.D. Noble, J.D. Way, B. Louie, Z.E. Reyes, B.R. Bateman, G.M. Horn and D.L. Reed, Inorg. Chem., 24 (1984) 1147.
5 M.R. Houchin, Inorg. Chim. Acta, 83 (1984) 103.
6 J. Takács and L. Markó, Trans. Met. Chem., 9 (1984) 10.
7 J. De Beer and R.J. Haines, J. Organomet. Chem., 36 (1972) 297.
8 M. Pankowski and M. Bigorgne, J. Organomet. Chem., 125 (1977) 231.
9 W. Hieber and K. Kaiser, Z. Naturforsch. B, 24 (1969) 778.
10 U. Berger and J. Strahle, Z. Anorg. Allg. Chem., 516 (1984) 19.
11 K. Edgar, B.F.G. Johnson, J. Lewis and S.B. Wild, J. Chem. Soc. A, (1968) 2851.
12 B. Demerseman, G. Bouquet and M. Bigorgne, J. Organomet. Chem., 35 (1972) 341.
13 P. Main (principal author), S.E. Hull, L. Lessinger, G. Germain, J-P. Declercq, and M.M. Woolfson, MULTAN 78, A System of Computer Programmes for the Automatic Solution of Crystal Structures from X-ray Diffraction Data (the Universities of York, England and Leuven, Belgium).
14 L Párkányi, K.H. Pannell and C. Hernandez, J. Organomet. Chem., 252 (1983) 127.